SPUTTERING MEASUREMENTS OF THE
CRITICAL ANGLE OF CHANNELING

by

JOHN ERIC NORBERG

B. S., Kansas State University, 1967

———————————

A MASTER'S THESIS

submitted in partial fulfillment of the

requirements for the degree

MASTER OF SCIENCE

Department of Physics

KANSAS STATE UNIVERSITY
Manhattan, Kansas

1969

Approved by

Major Professor

LD
2668
T4
1969
N65

TABLE OF CONTENTS

INTRODUCTION

Particles bombarding a single crystal have been found to exhibit anomalous behavior when incident along low index crystal directions. Energy loss has been shown to be unusually small in these directions and some of the projectiles penetrate to very great depths in the crystal. For many processes, such as sputtering and backscattering, which require a close encounter between projectiles and the atoms of the target crystal, minima occur when the projectile beam is aligned close to a low index direction. These phenomena indicate that part of the incident beam of particles have a lower limit imposed on the distance between themselves and the target atoms. This can be explained if the atoms of the rows in the low index directions provide a set of correlated collisions with the projectiles which steer them into the large open spaces or channels between the rows. In this way a portion of a beam of particles suffers only small changes of direction and travels directly into the crystal with a relatively small loss of energy.

A theory of channeling has been developed by Lindhard (1), which predicts the maximum angle a channeled particle can make with a low index crystal direction. The theory treats the problem in two approximations relevant to high and low particle energies.

The high energy expression for critical angle has been shown to agree with experiment by Davies (2). The low energy critical angle crudely agrees with the experimental results of Andreen and Hines (3). However, a close examination of this data showed that

the dependence on energy may be better explained by an alternative
expression which is examined in this thesis.

Onderdelinden (4) has been able to predict the sputtering
yield of single crystals with projectiles incident near the low
index crystal directions. Sputtering is assumed to be caused by
the energy loss of the unchanneled fraction of the beam in some
surface layer whose thickness is an adjustable parameter. On the
basis of the success of Onderdelinden's treatment, minima in sput-
tering yields are direct evidence of channeling.

In the present work, single crystals of silver, aluminum, and
gold were bombarded with ions ranging in atomic number from 1 to 18
and energy from 10 to 100 kev. The sputtering yield was measured
as a function of the angle between the ion beam and the $\langle 110 \rangle$ and
$\langle 100 \rangle$ crystal directions. The angular half widths at half minimum
of the sputtering yield were measured. The dependence of these
half widths upon energy, and atomic numbers, of the incident ions
and crystal atoms was compared to the values predicted by the low
energy theory of channeling.

THEORY

Some fraction of a perfectly collimated beam of energetic ions incident upon a perfect single crystal along a low index direction has small impact parameters with the crystal atoms at the surface. This fraction of the beam suffers large angle scattering and interacts with the crystal in a random way. The rest of the beam enters the relatively open spaces or channels bounded by atomic rows. The ions in this fraction of the beam will oscillate in the channels as they travel into the crystal. It is convenient to think of these as the aligned and random portions of the beam. If, as ions enter the crystal at some small angle to a channel direction, the energy in the motion transverse to the channel direction is less than the potential barriers of the channel boundaries, these ions will be trapped in the channel as they travel into the crystal.

For purposes of studying channeling, the atomic rows may be approximated by continious strings. The potential, $U(r)$, of such a string is the sum of the potentials of all the atoms in the row averaged over the atomic spacing in the row.

$$U(r) = \frac{1}{d} \int_{-\infty}^{\infty} V\left[\sqrt{r^2 + z^2}\right] dz \qquad (1)$$

r is the perpendicular distance from a field point to the row, d is the distance between atoms in a row, z is the distance along the row, and $V\left[(r^2 + z^2)^{\frac{1}{2}}\right]$ is the interaction potential between the ion and an isolated atom of the crystal. The collision between an ion and a string is assumed to be independent of the neighboring strings.

This string approximation requires that the ion undergo cor-
related collisions with the atoms in the row in the process of
being steered back into the channel. If an ion did not follow the
trajectories of the channeled ions, it would interact with an in-
dividual atom in the string for a time

$$\Delta t = \frac{r_{min}}{v \sin \psi} \ .$$

r_{min} is the distance of closest approach of channeled ions to the
string, and ψ is the angle between the velocity of the ion and the
channel direction at the center of the channel. The validity of
the string approximation requires that the distance traveled by an
ion parallel to the channel in this time be greater than the spacing
of the atoms in the row. Since the velocity parallel to the channel
direction is $v \cos \psi$, this condition gives

$$\frac{r_{min} \ v \ \cos \psi}{v \sin \psi} \ > \ d \ .$$

For small ψ this becomes

$$r_{min} \ > \ \psi d \tag{2}$$

The motion of a channeled ion can be projected onto a plane
normal to the string direction. The trajectory of the ion in this
plane will have an impact parameter l with the string. For any
particular values of ψ and ion energy E, the value of r_{min} will be
the smallest when $l = 0$. This situation is the most restrictive
case of (2) and requires that the kinetic energy in the normal
plane, E_t, becomes zero at r_{min}. The expression for the critical
angle is developed for the $l = 0$ case.

The energy balance for transverse motion is given by

$$E_t + U(r) = E \psi^2$$

At the minimum distance of approach and for small angles this becomes

$$U(r_{min}) = E\psi^2$$

(3)

Using some appropriate form of string potential and the inequality (2) to eliminate r_{min}, it is possible to obtain an estimate for a maximum angle at which channeling can occur. Lindhard (5) has used this method to develop expressions for the critical angle in the cases of high and low energy channeling.

Lindhard's treatment of high energy channeling, based on a Thomas-Fermi atom-atom potential, uses

$$U(r) = \frac{Z_1 Z_2 e^2}{d}\left[2 \ln \frac{Ca}{r}\right]$$

where the screening length a is $\frac{(0.8853) a_0}{\left[Z_1^{2/3} + Z_2^{2/3}\right]^{1/2}}$ and a_0 is the

Bohr radius. This is a reasonable approximation to the string potential for r < a. C is a constant of integration which appears in a general expression for the string potential given by Lindhard and is assigned the value $\sqrt{3}$.

Using the relations (2) and (3), r_{min} is eliminated with the result

$$\frac{Z_1 Z_2 e^2}{d} 2 \ln \frac{Ca}{d\psi} > E\psi^2.$$

This can be rewritten as

$$\frac{Ca}{d\psi} \exp\left[\frac{-\psi^2 d}{2b}\right] > 1 ,$$

where $b = \frac{Z_1 Z_2 e^2}{E}$. If the inequality holds for very small it will be violated first by the exponential as ψ is increased.

Extremely small values of the exponential can be eliminated by requiring $\psi^2 < \frac{2b}{d}$. The inequality will hold then if $\frac{ca}{\psi d} > e$. The first of these gives an estimate of the critical angle.

$$\psi < \psi_1 = \sqrt{\frac{2b}{d}} = \left[\frac{2 Z_1 Z_2 e^2}{E d}\right]^{1/2} \qquad (4)$$

The second provides limitations on the energy region in which the treatment is valid. $\frac{a}{d} > \psi_1 \frac{e}{C}$. Since $\frac{e}{\sqrt{3}} > 1$, this becomes

$$\frac{a^2}{d^2} > \frac{2 Z_1 Z_2 e^2}{E d} \quad \text{or} \quad E > E' = \frac{2 Z_1 Z_2 e^2 d}{a^2} \qquad (5)$$

Smaller energies result in larger values of r_{min}. For this reason Lindhard uses an approximation to the string potential that is valid in a region $r > Ca$,

$$U(r) = \frac{Z_1 Z_2 e^2}{d} \left[\frac{Ca}{r}\right]^2 .$$

Using (2) and (3) to eliminate r_{min}, the relation

$$\frac{(Ca)^2}{d^3} b > \psi^4$$

is obtained. This can be written as

$$\psi < \psi_2 = \left[\frac{Ca b^{1/2}}{d d^{1/2}}\right]^{1/2} = \left[\frac{Ca}{\sqrt{2} d} \psi_1\right]^{1/2} = \left[\frac{(Ca)^2}{d^3} \frac{Z_1 Z_2 e^2}{E}\right]^{1/4} . \qquad (6)$$

Since the approximation to the string potential was based on $r > Ca$, it follows that $r_{min} > Ca$. In so far as (2) becomes $r_{min} = \psi_2 d$, the relation $\psi_2 > \frac{a}{d}$ gives a limitation on the energy region to which this treatment should apply. Since $\frac{C}{\sqrt{2}} \approx 1$, the last inequality can be written as $\frac{a}{d} \psi_1 > \left[\frac{a}{b}\right]^2$. With the expression for ψ_1 this becomes .

$$\frac{2 Z_1 Z_2 e^2}{E d} > \left[\frac{a}{d}\right]^2 ; \quad \frac{2 Z_1 Z_2 e^2 d}{a^2} > E ; \quad E < E' .$$

Lindhard has developed these two cases to give estimates of the behavior of the critical angle for channeling. The expressions for ψ_1, and ψ_2 are critical angles in the sense that particles in the aligned portion of a beam make angles ψ with the channel axis such that $\psi < C'\psi_1$ or $\psi < C'\psi_2$. The constant C', which Lindhard uses, is between 1 and 2.

Both expressions for the critical angle predict dependence on the energy, atomic numbers of the incident particles and target atoms, and lattice spacing of the crystal. These treatments deal with interactions occuring at ranges such that $r < a$ in the high energy case and $r > Ca$ in the low energy case. It is interesting to consider the effects of interactions occuring in the neighborhood of $r=a$.

Moliere (6) has given an approximation to the Thomas-Fermi potential with the form

$$V(r) = \frac{Z_1 Z_2 e^2}{R}\left[0.1 \exp\left(-\frac{6R}{a}\right) + 0.55 \exp\left(-\frac{1.2R}{a}\right) + 0.35 \exp\left(-\frac{0.3R}{a}\right)\right].$$

This approximation has been used by Erginsoy (7) to develop an expression for the string potential.

$$U(r) = \frac{2Z_1 Z_2 e^2}{d}\left[0.1 K_0\left(\frac{6r}{a}\right) + 0.55 K_0\left(\frac{1.2\,r}{a}\right) + 0.35 K_0\left(\frac{0.3\,r}{a}\right)\right] \quad (7)$$

The functions K_0 which appear in this expression are modified Bessel functions of the second kind. In the neighborhood of $r=a$, the string potential can be reduced to

$$U(r) = \frac{B\,\pi a Z_1 Z_2 e^2}{r\,d}, \quad (8)$$

with the use of polynomial approximations to K_o, Abramowitz and Stegun (8). B is a constant on the order of 0.5. Using this expression for the string potential and the requirements for channeling (2) and (3), an expression for the critical angle was developed.

$$\frac{B\pi a Z_1 Z_2 e^2}{\psi d^2} > E\psi^2$$

This can be rewritten as

$$\psi < \psi_c = \left[\frac{B\pi a Z_1 Z_2 e^2}{Ed^2}\right]^{1/3} \tag{9}$$

For ease of comparison the expressions for ψ_1 and ψ_2 are listed again.

$$\psi_1 = \left[\frac{2Z_1 Z_2 e^2}{Ed}\right]^{1/2} \tag{4}$$

$$\psi_2 = \left[\frac{3a^2 Z_1 Z_2 e^2}{Ed^3}\right]^{1/4} \tag{6}$$

Whenever Z_1 is much less than Z_2, the screening length reduces to

$$a = \frac{0.8853\, a_o}{Z_2^{1/3}} \ .$$

With this approximation the dependence of critical angle on Z_1 or Z_2 has a much more simple form.

The predicted dependences on E, Z_1, and Z_2 are summarized in Table I for ψ_1 , ψ_2 , and ψ_c .

EXPLANATION OF PLATE I

Table I. A summary of the behavior of the
critical angle predicted by ψ_1,
ψ_2, and ψ_c.

PLATE I

TABLE I

Dependence of ψ_1, ψ_2, and ψ_c, on E, Z_1, and Z_2.

Critical Angle	E	Z_1	Z_2
ψ_1	$E^{-1/2}$	$Z_1^{1/2}$	$Z_2^{1/2}$
ψ_2	$E^{-1/4}$	$Z_1^{1/4}$	$Z_2^{1/12}$
ψ_c	$E^{-1/3}$	$Z_1^{1/3}$	$Z_2^{2/9}$

SPUTTERING

The developments of the critical angles for channeling have all used the basic assumption than the channeled particles approach no closer than some minimum distance to the atoms of the target. This assumption is well justified by experiments which measure secondary processes which depend on the close approach of a projectile. Such experiments have shown minima in backscatter yield and yields for various nuclear processes when particles bombarding a single crystal were incident in a channeling direction. Similar minima have been observed in sputtering yields.

Onderdelinden (9) has been able to calculate sputtering yield as a function of ψ by assuming that it is proportional to the energy lost by the nonaligned portion of a beam of particles within a certain depth, x_0, of the target.

These calculations were first performed for a beam of particles parallel to a channeling direction, with the proportionality constant and x_0 as adjustable parameters. The results were compared with measured values of the sputtering yield at various energies in order to fix the parameters. Using these parameters and estimates of the nonaligned portion of the beam based on Lindhard's low energy critical angle, Onderdelinden was able to calculate the dependence of the sputtering yield on the angle between the channel and the beam. These calculations were found to be in good agreement with experimental data.

The success of Onderdelinden's method of calculating sputtering yield indicates that sputtering yield is a good measure of

channeling. In the course of his development, Onderlinden found that x_0 was on the order of 100 $\overset{\circ}{A}$, so that sputtering measures channeling at the surface of the crystal. Backscatter studies by Davies (10) indicate that the critical angle is a function of depth and temperature in the target. However, the critical angle was shown to be insensitive to temperature at the surface. Therefore, sputtering measurements provide a method to study channeling at the surface of a single crystal and eliminate problems associated with temperature.

Plate II illustrates the energy and temperature dependence of sputtering yield. Almen and Bruce (11) found that over the energy range studied, the sputtering yield was fairly large. This allows measurements to be made with low beam currents to minimize crystal damage. The stability of the sputtering yield observed by Nelson (12) in the neighborhood of ambient temperatures is another factor in the desirability of sputtering measurements from the experimental point of view.

EXPLANATION OF PLATE II

Fig. 1. The sputtering yield of Ag bombarded
        by Ar, Ne, and N at various energies.

Fig. 2. The behavior of the sputtering yield
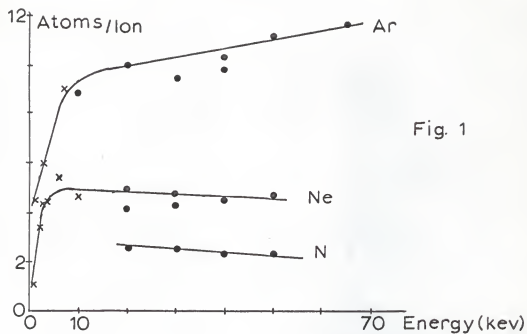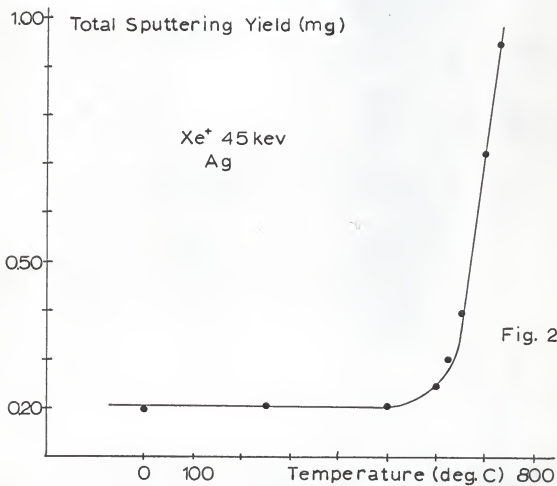   of Ag with temperature.

PLATE II

Fig. 1

Fig. 2

EXPERIMENTAL METHOD

Sputtering measurements were made with Au, Al and Ag single crystals. These crystals were produced by Semi-elements, Inc., and were grown to a size of about 0.5" x 0.5" x 0.25" with the ⟨111⟩ direction normal to the surface. All of these crystals have fcc structure with lattice spacings of 4.04Å, 4.07Å, and 4.08Å for Al, Au, and Ag respectively.

The crystals were rotated about an axis parallel to the ⟨111⟩ direction as shown in Plate III. This rotation was monitored and recorded as the angle ϕ. The ϕ axis was set at an angle, Θ, to the ion beam equal to the angle between the ⟨111⟩ direction and the channel direction to be studied. The ϕ rotation was continuously driven by a motor so that the desired channel direction was rotated through the ion beam.

The charge given off by the crystal was collected with a large plate subtending a solid angle of about 2π steradians at the crystal surface. The current between the collector and ground was measured by a Keithley Picoammeter. The collector plate could be biased with respect to the crystal. With the ion beam striking the crystal in a random direction, the measured current was recorded for various biasing voltages. This data was plotted as current yield, measured current divided by incident ion current, versus biasing voltage. Plate IV shows the results for a beam of $^4\text{He}^+$ ions bombarding a gold crystal. The positive yield quickly stabilized to a value of R^+ on the order of 1, near a biasing voltage of -20 volts. R^+ could be composed of backscattered positive ions,

EXPLANATION OF PLATE III

A schematic representation of the orientation
of the crystal in the target chamber with re-
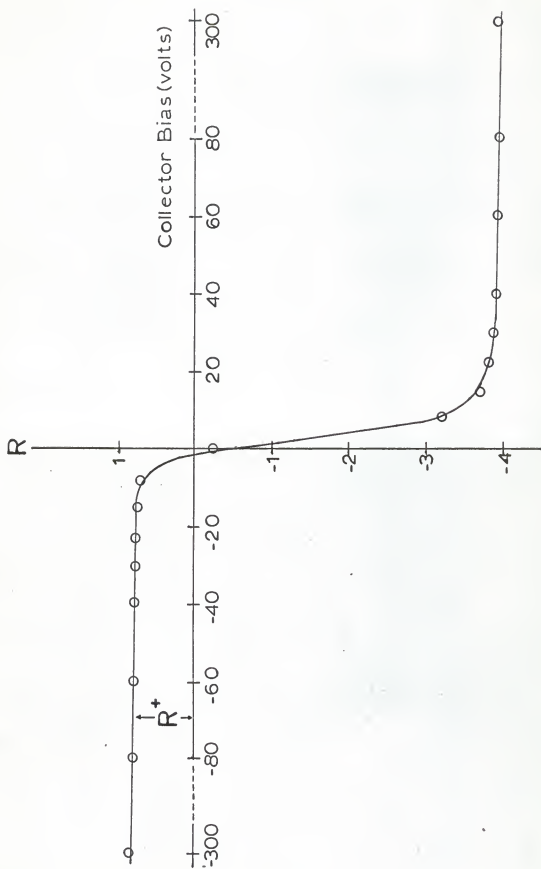spect to the ion beam and the collector.

PLATE III
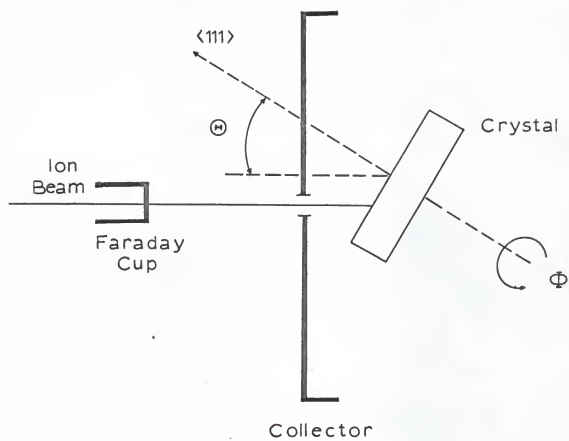
EXPLANATION OF PLATE IV

The total current between the collector plate and ground divided
by the current of the incident ions as a function of the bias
between the collector and the crystal.

PLATE IV

secondary electrons ejected from the collector plate by the ener-
getic backscattered particles, or positively charged sputtered
target atoms. However, estimates of the backscatter yield in this
energy region are on the order of 10^{-3}. Therefore, backscattered
ions and their secondary electrons can be ignored in R^+. All sput-
tering measurements were taken at a collector bias of about -70
volts.

Sputtering yield, R^+, was recorded as a function of ϕ, on a
Brush strip chart recorder, and minima were observed to be centered
about ϕ values that correspond to low index crystal directions.
This data was taken for the $\langle 100 \rangle$ and $\langle 110 \rangle$ directions in all three
crystals. Beam currents and sputtering currents were on the order
of 10^{-10} amperes. The crystals were bombarded with ions from H^+
to Ar^+ with energies from 10 to 100 kev. The energy of the ion
beam was uncertain by 2%.

Examples of the sputtering yield minima are shown in Plate V.
Three distinct minima were observed for each revolution of the
crystal. This is caused by threefold symmetry about the $\langle 111 \rangle$
direction. Ninety degree increments of ϕ were marked on the strip
chart recorder. The linear half width at half minimum of the
sputtering minima were measured and converted to an angular measure
of ψ.

According to Onderdelinden's treatment of sputtering, the
half minimum of the sputtering yield corresponds to a situation in
which the aligned fraction of the beam is one half of that value
it would have for $\psi=0$. The sputtering yield apptoaches the base
line for random direction sputtering as ψ approaches the critical

EXPLANATION OF PLATE V

Three examples of the recorder output with 90°
incriments of ϕ indicated. The large minima
represent channeling in the direction consid-
ered in each case. The smaller minima corre-
spond to other channeling directions.

Fig. 3. Collected current for 45 kev H^{+} ions
         incident upon the $\langle 100 \rangle$ direction in Ag.

Fig. 4. Collected current for 25 kev Ne^{+} ions
         incident upon the $\langle 100 \rangle$ direction of Ag.

Fig. 5. Collected current for 100 kev N^{+} ions
         incident upon the $\langle 110 \rangle$ direction of Ag.

PLATE V

Fig. 3

Fig. 4

Fig. 5
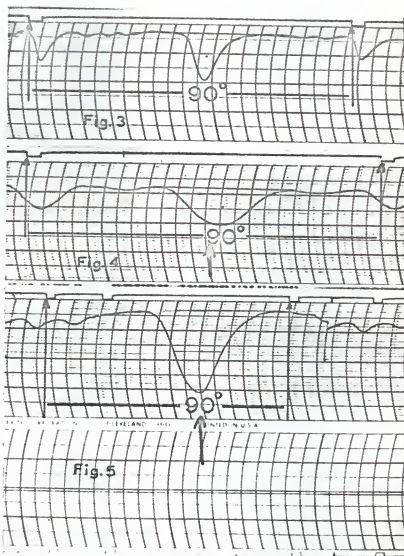
angle. In addition the angular divergence and small energy spread
of the ion beam make the intersection of the minimum with the base
line an unreliable measure of the critical angle. The width of
the sputtering yield minimum at half minimum is distinct and rel-
atively insensitive to the angular divergence and energy spread of
the beam. For these reasons the critical angle was not measured
directly, but $\psi_{\frac{1}{2}}$, the half width at half minimum of the sputter-
ing yield, was used to determine its dependence on E, Z_1, and Z_2.

It was observed that the three minima in a single rotation
did not have the same shape. This indicated that the ϕ axis was
not truly parallel to the ⟨111⟩ direction in the crystal. As the
crystal was rotated, each of the three equivalent channeling di-
rections made slightly different angles with the ion beam. This
problem was attributed to errors in mounting the crystals and in-
accuracies in the crystal surface. It was necessary to observe
the behavior of one of the three minima for various Θ settings.
A value of Θ was selected for this minimum between extremes of
misalignment with consideration for depth, width, and symmetry of
the minimum.

Several measurements of the sputtering yield were taken for
each selected channel at a particular energy. The measured half
widths were averaged to obtain mean values which were found to be
reproducible to within 3%. The angular widths of the sputtering
minima in terms of the angle ψ between the ion beam and the chan-
nel direction were calculated from the relation $\psi_{\frac{1}{2}} = \phi_{\frac{1}{2}} \sin \Theta$.
This relation is easily derived from the geometry of the crystal
mounting.

APPARATUS

The main elements of the apparatus are shown in Plate VI. The desired ions were produced from their elemental gaseous state in the ion source. These ions were drawn into the accelerating tube by an extraction electrode and accelerated to a predetermined energy. The ion beam was defined by a 1 mm slit S_1. Since the energy of the ions was known, the bending magnet was used to select the desired mass by assuming charge states of +1.

The ion beam was collimated by two 1.5 mm slits, S_2 and S_3, separated by a distance of one meter. The angular divergence of the beam was less than $\pm 0.09^{\circ}$. The pressure above S_1 was about 10^{-5} torr, and between S_2 and S_3 it was about 10^{-6} torr. The vacuum in the target chamber was maintained at about 10^{-8} torr by the two Ultek Differential Sputtering ion pumps. A Faraday cup behind S_3 could be moved into the beam to measure the incident ion current. The ϕ rotation was monitored by the use of four electrical contacts which sent a voltage pulse to the recorder at each 90° increment. An adjustable pot well insulated from ground was used to bias the collector. The Keithley Model 416 Picoammeter has a rise time of less than 0.04 sec. in the current range used, and is equipped with a 3 volt recorder output. This was used to drive the Brush strip chart recorder, so that a continuous record of the sputtering current with each 90° increment of ϕ denoted was obtained.

EXPLANATION OF PLATE VI

The main features of the apparatus used to
make the ion beam and measure the sputtering
yield.

PLATE VI
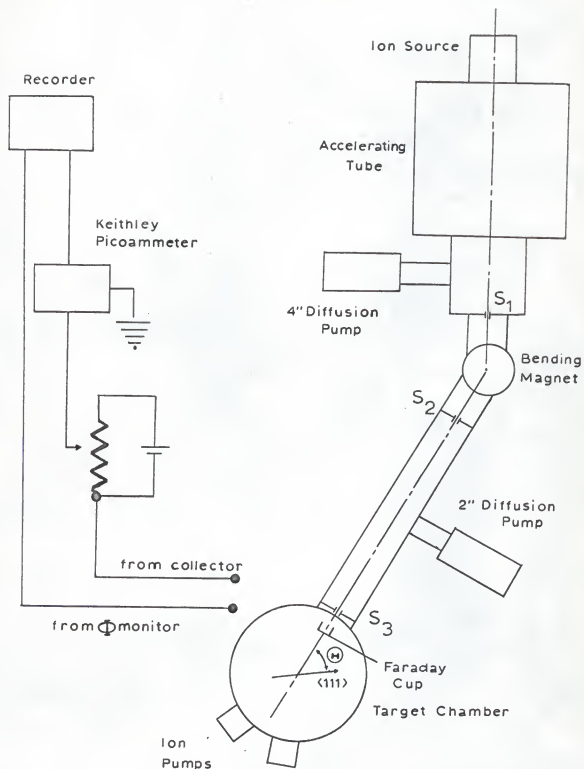
RESULTS

The observed dependence of $\psi_{\frac{1}{2}}$ on energy for various pro-
jectiles in Ag is displayed in Plates VII and VIII. If the de-
pendence is of the form $\psi_{\frac{1}{2}} \propto E^{-p}$, with p a constant, a log-log
plot of $\psi_{\frac{1}{2}}$ versus E will be a straight line of slope -p. It was
found that straight lines were a good fit to this data in all
cases. The slopes are listed in Table II. The energy E' which
divides Lindhard's development into high and low energy regions is
also listed in Table II. A 3% uncertainty in $\psi_{\frac{1}{2}}$ makes the slopes
uncertain by $\pm$ 0.03.

TABLE II

Measured slopes of log-log plots of $\psi_{\frac{1}{2}}$
versus E and calculated values of E'.

Projectile	Slope	E'(kev)
100 direction		
H^+	-0.38	346
He^+	-0.38	885
N^+	-0.29	2890
Ne^+	-0.30	4360
110 direction		
H^+	-0.44	245
He^+	-0.42	626
N^+	-0.33	2043
Ne^+	-0.32	3081
Ar^+	-0.24	4360

EXPLANATION OF PLATE VII

The energy dependence of the critical angle for various ions bombarding Ag near the ⟨110⟩ direction. The data is displayed on a log-log plot.
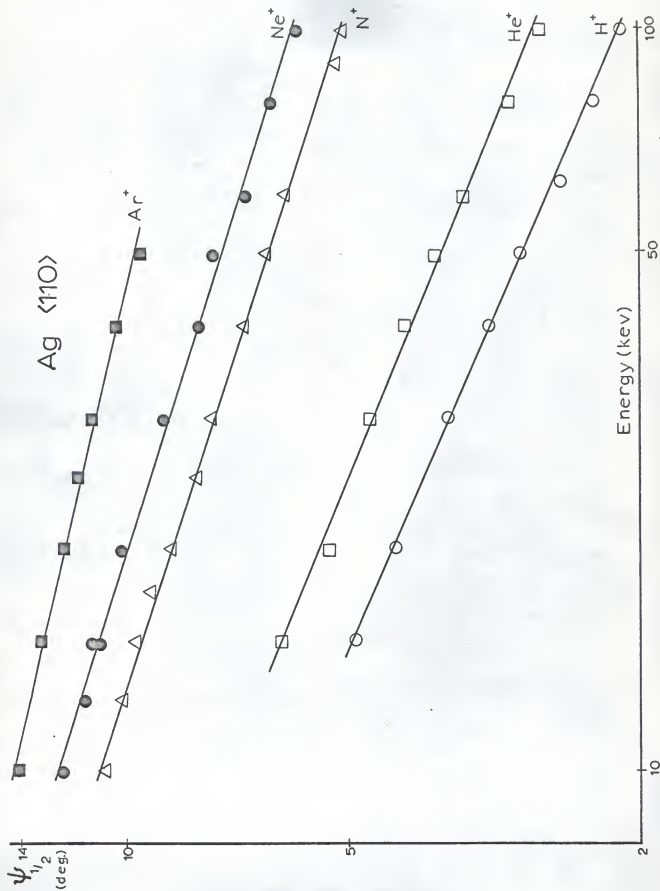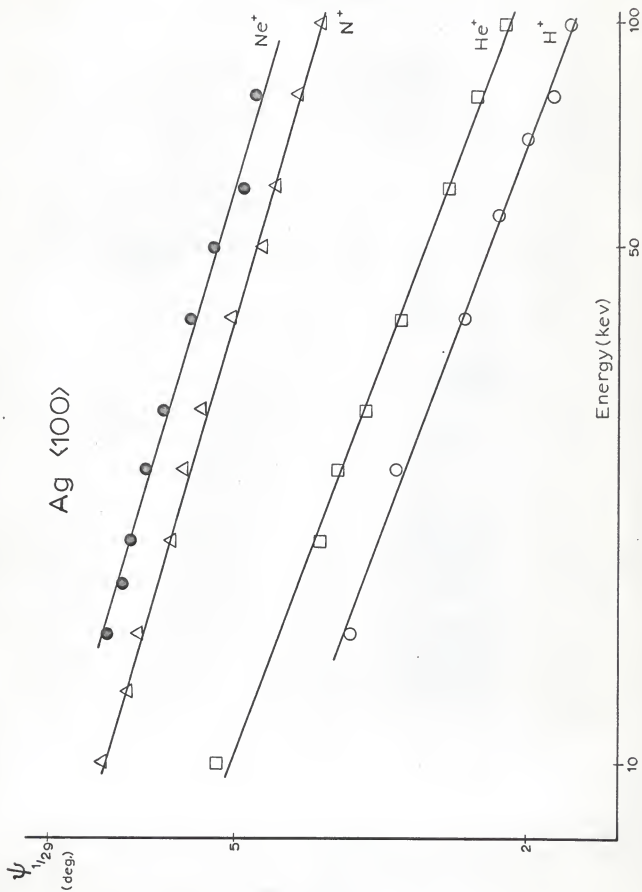
PLATE VII

EXPLANATION OF PLATE VIII

The energy dependence of the critical angle for various ions bombarding Ag near the ⟨100⟩ direction. The data is displayed on a log-log plot.

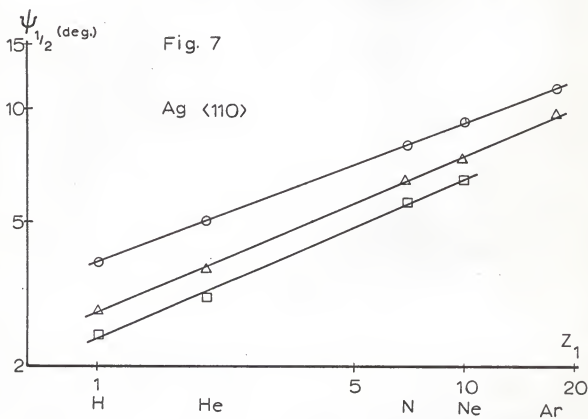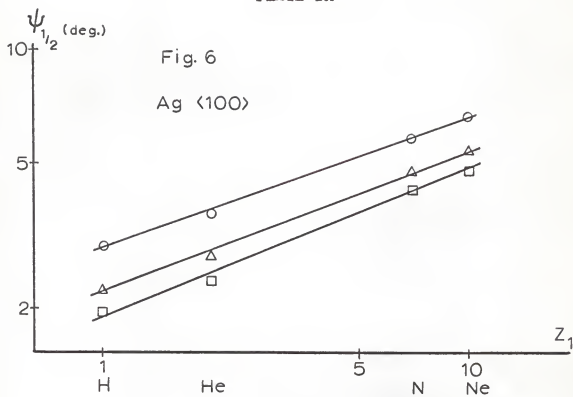PLATE VIII

EXPLANATION OF PLATE IX

The dependence of $\psi_{\frac{1}{2}}$ on Z_1 in Ag. The data
is displayed on log-log plots.

      ○   Denotes 25 kev

      △   Denotes 50 kev

      □   Denotes 75 kev

PLATE IX

Fig. 6

Ag ⟨100⟩

Fig. 7

Ag ⟨110⟩

EXPLANATION OF PLATE X

The dependence of $\psi_{\frac{1}{2}}$ on Z_2 in the $\langle 110 \rangle$ direction of Ag. The data is displayed on log-log plots.

Fig. 8. He^+ incident ions.

Fig. 9. H^+ incident ions.

        ◯   Denotes 25 kev

        △   Denotes 50 kev

        □   Denotes 75 kev

PLATE X

Fig. 8

$\psi_{1/2}$ (deg.)

He$^+$ ⟨110⟩

Fig. 9

$\psi_{1/2}$ (deg.)

H$^+$ ⟨110⟩

EXPLANATION OF PLATE XI

The dependence of $\psi_{\frac{1}{2}}$ on Z_2 in the $\langle 100 \rangle$ direction of Ag. The data is displayed on log-log plots.
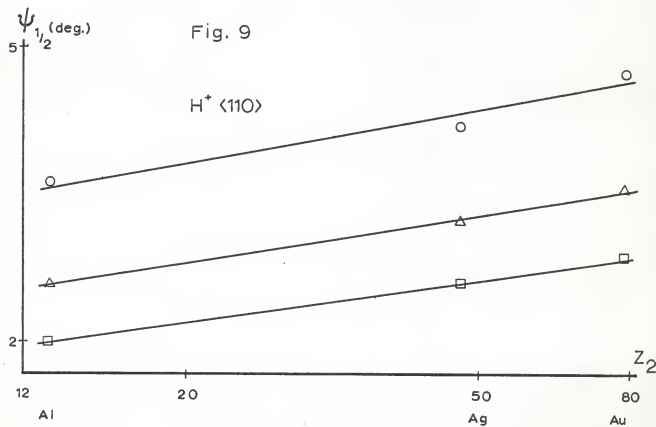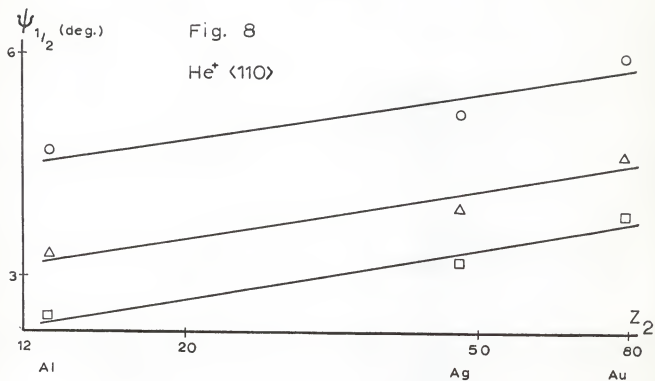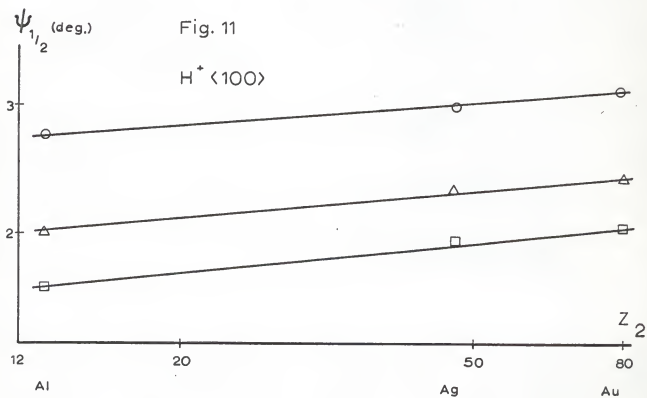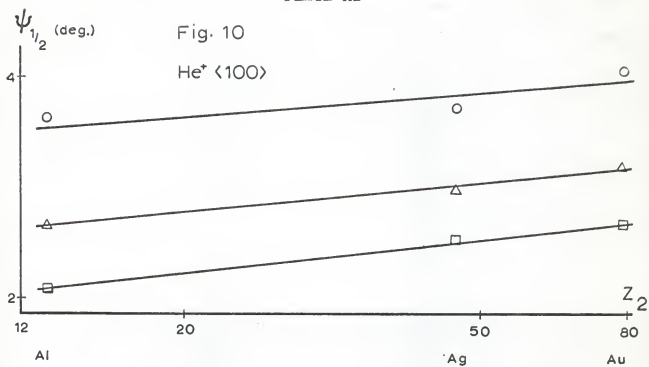
Fig. 10. He^+ incident ions.

Fig. 11. H^+ incident ions.

Denotes 25 kev

Denotes 50 kev

Denotes 75 kev

PLATE XI

Fig. 10

$\psi_{1/2}$ (deg.)

He$^+$ ⟨100⟩

Fig. 11

$\psi_{1/2}$ (deg.)

H$^+$ ⟨100⟩

The energy region studied was in all cases below E', and the observed slopes fall in a range between -0.24 and -0.44. The steepest slopes were observed for H^+ and He^+ which also have the lowest values of E'.

The assumption that Z_1 is much less than Z_2 made it possible to describe the dependence of ψ_1, ψ_2, and ψ_c upon Z_1 and Z_2 as a simple power law. This predicted behavior was summarized in Table I. The slopes of straight lines fitted to log-log plots of $\psi_{\frac{1}{2}}$ vs Z_1 and $\psi_{\frac{1}{2}}$ vs Z_2 were measured to study the dependence of the critical angle on Z_1 and Z_2.

The measured values of $\psi_{\frac{1}{2}}$ are plotted against Z_1 in Plate IX for various ion energies in Ag. Straight lines provided a good fit to this data, and the slopes are listed in Table III. These slopes are uncertain by ±0.02 for the ⟨110⟩ data and ±0.03 for the ⟨100⟩ data.

TABLE III

Measured slopes of $\psi_{\frac{1}{2}}$ versus Z_1

Energy (kev)	Slope
⟨100⟩ direction	
25	0.39
50	0.39
75	0.41
⟨110⟩ direction	
25	0.37
50	0.42
75	0.43

The Z_2 dependence of the critical angle was studied with H^+ and He^+ ions bombarding Au, Ag, and Al. Log-log plots of $\psi_{\frac{1}{2}}$ versus Z_2 appear in Plate X and Plate XI. The slopes of straight lines fitted to the three points obtained for each energy are listed in Plate XII. The slopes of these lines were uncertain by ± 0.03.

The spacing of atoms in the $\langle 110 \rangle$ row, d_{110}, is equal to $(2)^{-\frac{1}{2}}$ of the spacing in the $\langle 100 \rangle$ row d_{100}. The ratio of the critical angles $\psi_c\langle 110 \rangle / \psi_c\langle 100 \rangle$ with Z_1, Z_2, and E fixed is $(2)^{1/3}$ or about 1.26. These ratios were calculated for H^+, He^+, N^+, and Ne^+ on Ag for energies of 25, 50, and 75 kev. The results are summarized in Table IV, and the average value was found to be 1.34.

TABLE IV

Measured values of the ratio $\psi_c\langle 110 \rangle / \psi_c\langle 100 \rangle$

Energy (kev)	Projectile:	H^+	He^+	N^+	Ne^+
25		1.32	1.39	1.39	1.40
50		1.22	1.34	1.36	1.39
75		1.23	1.31	1.34	1.38

In order to compare the three expressions for the critical angle with the observed behavior of $\psi_{\frac{1}{2}}$, the predicted dependences of ψ_1, ψ_2, and ψ_c on Z_1, Z_2 and E are summarized in Table VI along with the range of observed dependences.

EXPLANATION OF PLATE XII

Table V. The slopes of the $\psi_{\frac{1}{2}}$ vs Z_2 plots.
These slopes were measured from the
graphs in Plate IX and Plate X.

PLATE XII

TABLE V

Measured value of the slope $\psi_{\frac{1}{2}}$ versus z_2

Energy (kev)	Slope
⟨110⟩ direction	
H^+	
25	0.19
50	0.16
75	0.15
He^+	
25	0.15
50	0.16
75	0.17
⟨100⟩ direction	
H^+	
25	0.07
50	0.09
75	0.10
He^+	
25	0.08
50	0.10
75	0.11

EXPLANATION OF PLATE XIII

Table VI. Listings of the dependence of ψ_1, ψ_2, and ψ_c and the observed dependence of $\psi_{\frac{1}{2}}$ on E, Z_1, and Z_2.

PLATE XIII

TABLE VI

Predicted and observed dependence

	ψ_1	ψ_2	ψ_c	Range of Observed Values	
Energy Dependence	-0.50 E	-0.25 E	-0.33 E	-0.29 to -0.38 E	$\langle 00 \rangle$
				-0.24 to -0.44 E	$\langle 10 \rangle$
Z_1 Dependence	$0.50\ Z_1$	$0.25\ Z_1$	$0.33\ Z_1$	$0.39\ Z_1$ to $0.41\ Z_1$	$\langle 00 \rangle$
				$0.37\ Z_1$ to $0.43\ Z_1$	$\langle 10 \rangle$
Z_2 Dependence	$0.50\ Z_2$	$0.08\ Z_2$	$0.22\ Z_2$	$0.07\ Z_2$ to $0.11\ Z_2$	$\langle 00 \rangle$
				$0.15\ Z_2$ to $0.19\ Z_2$	$\langle 10 \rangle$

CONCLUSIONS

The experimental results show that in the energy range stud-
ied, the critical angle for channeling can be described by a re-
lationship of the form $\psi_c \propto E^{-p}$ for various values of p. It was
found that p tended to decrease as E', the dividing point between
Lindhard's high and low energy regions, increased.

The data summarized in Table VI show that for the range of
ions studied, ψ_c best describes the energy dependence of the crit-
ical angle. In the extreme cases, the energy dependence was found
to be $E^{-0.24}$ and $E^{-0.44}$. These values bracket the behavior pre-
dicted by ψ_c, but are outside the estimated uncertainty ±0.03.
These results indicate that ψ_c gives a reasonable approximation
to the energy dependence of the critical angle for the ions stud-
ied in the energy range 10 to 100 kev.

The Z_1 dependence of the critical angle was found to be pro-
portional to $Z_1^{p_1}$. The observed values of p_1 were all between
0.37 and 0.43. This behavior is about midway between 0.33 pre-
dicted by ψ_c and 0.50 predicted by ψ_1. However, both of these
predicted values are outside the estimated uncertainty which was
±0.03.

Only crude estimates of the Z_2 dependence of the critical
angle were possible. Straight lines fitted to the three points
plotted for each case showed a definite difference in slope for
the ⟨100⟩ and ⟨110⟩ directions. Assuming a dependence of the form
$Z_2^{p_2}$, the observed values of p_2 in the ⟨100⟩ direction were be-
tween 0.07 and 0.11. These agree with the dependence predicted

by ψ_2, 0.08, within the estimated uncertainty ±0.03. The range of p_2 in the ⟨110⟩ direction was 0.15 to 0.19. These values fall closer to the prediction of ψ_c which is 0.22. However, only the largest is within the estimated uncertainty.

It was found that none of the expressions for the critical angle could consistantly predict the dependence on the atomic numbers of the incident ions and crystal atoms.

ACKNOWLEDGMENT

LITERATURE CITED

1. Lindhard, J., Kgl. Danske Videnskab Selskab, Mat. Fys. Medd., $\underline{34}$, No. 14 (1965)

2. Davies, J., J. Denhartog, and J. L. Whitton, Phys. Rev., $\underline{165}$, 345 (1968)

3. Andreen, C. J., and R. L. Hines, Phys. Rev., $\underline{159}$, 285 (1967)

4. Onderdelinden, D., Can. J. Phys., $\underline{46}$, 739 (1968)

5. Lindhard, J., loc. cit.

6. Moliere, G., A. Naturforsch, $\underline{2a}$, 133 (1947)

7. Erginsoy, C., Phys. Rev. Letters, $\underline{15}$, 360, (1965)

8. Abramowitz, M., and I. A. Stegun ed., Handbook of Mathematical Functions, p379, (1965) Dover, Publications, Inc., New York

9. Onderdelinden, D., loc. cit.

10. Davies, J., J. Denhartog, and J. L. Whitton, loc. cit.

11. Almen, O. D., and G. Bruce, Nucl. Inst. Meth., $\underline{11}$, 257 (1961)

12. Nelson, R. S., Phil. Mag., $\underline{11}$, 291 (1965)

SPUTTERING MEASUREMENTS OF THE
CRITICAL ANGLE FOR CHANNELING

by

JOHN ERIC NORBERG

B. S., Kansas State University, 1967

_____

AN ABSTRACT OF A MASTER'S THESIS

submitted in partial fulfillment of the

requirements for the degree

MASTER OF SCIENCE

Department of Physics

KANSAS STATE UNIVERSITY
Manhattan, Kansas

1969

The angular widths of minima in sputtering yield were used to study the critical angle for channeling in the $\langle 100 \rangle$ and $\langle 110 \rangle$ directions in fcc crystals. Silver, aluminum, and gold single crystals were bombarded with ions ranging from H^+ to Ar^+ at energies between 10 and 100 kev. The dependence of the critical angle on incident ion energy E and the atomic numbers of the incident ions and the crystal atoms was measured and compared with theoretical predictions.

Three expressions for the critical angle were given. Two of these, ψ_1 and ψ_2, were developed by Lindhard for cases of high and low energy channeling. The third ψ_c was based on the Moliere atom-atom potential.

The crystals were rotated about the $\langle 111 \rangle$ direction which was normal to the crystal surface. The $\langle 111 \rangle$ direction was set at an angle to the ion beam equal to the angle between the $\langle 111 \rangle$ direction and the channeling direction. The charge liberated from the crystal under ion bombardment was used to measure the sputtering yield as a function of the angle between the ion beam and a channeling direction. The angular half widths at half minimum of the minima in the sputtering yield were plotted on log-log graphs to measure a power law dependence of the critical angle on E, Z_1, and Z_2. Straight line fits to these plots showed that a power law was a good description of the E and Z_1 dependence. The three points of each Z_2 dependence plot were in reasonable agreement with a straight line.

The observed powers in the energy dependence fell between -0.24 ± 0.03 and -0.44 ± 0.03. These were best predicted by ψ_c

with a dependence of $E^{-0.33}$. The Z_2 dependence in the $\langle 100 \rangle$ channel direction was in good agreement with ψ_2. In the $\langle 110 \rangle$ direction the Z_2 dependence was found to be midway between the behavior predicted by ψ_0 and ψ_1. Thus the dependence of critical angle on Z_1 and Z_2 cannot be consistently described by any of the three theoretical expressions considered.